

Half-Metallic Ferrimagnetism in Mn_2VAl

Ruben Weht and Warren E. Pickett

Department of Physics, University of California, Davis CA 95616

(March 14, 2018)

We show that Mn_2VAl is a compound for which the generalized gradient approximation (GGA) to the exchange-correlation functional in density functional theory makes a qualitative change in predicted behavior compared to the usual local density approximation (LDA). Application of GGA leads to prediction of Mn_2VAl being a half-metallic ferrimagnet, with the minority channel being the conducting one. The electronic and magnetic structure is analyzed and contrasted with the isostructural enhanced semimetal Fe_2VAl .

I. INTRODUCTION

The cubic Heusler structure class X_2YZ of inter-metallic compounds provides a great variety of behavior, including an interesting variety of magnetic phenomena. A striking example is the prediction, solely from band theory, of half-metallic (HM) ferromagnetism (FM) in this class (and the related half-Heuslers XYZ). [1]

In the Heusler systems HM FM has never been unambiguously confirmed by experiment, although there is strong evidence in some cases. Only in the “colossal magnetoresistance” system $\text{La}_{1-x}\text{Sr}_x\text{MnO}_3$ have HM signatures been seen directly and clearly in spin-polarized photoemission experiments, [2] as was predicted from band theory calculations utilizing the local density approximation (LDA) [3] for the exchange-correlation energy functional. Probably several Heusler and half-Heusler compounds are HM.

Over the past fifteen years many (probably at least twenty) HM FM compounds have been predicted based on LDA, and there has not been much reason to doubt the computational results (for example, these are not strongly correlated materials). Recent examples include $\text{Sr}_2\text{FeMoO}_6$, which appears to be supported by experimental data, [4] and possible HM materials with vanishing moment – “HM antiferromagnets” – which have not yet been made. [5] However, there is a need to make predictions as robust as possible, and in the double perovskite structure of $\text{Sr}_2\text{FeMoO}_6$ and the proposed HM antiferromagnets structural distortions are a likely occurrence and cloud the forecasts based on an ideal structure. The Heusler structure we consider here are much less inclined to distortion, [6] leaving the prediction based solely on the quality of the electronic structure description.

Here we present a case of a Heusler structure compound where the use of the generalized gradient approximation (GGA) [7] to the exchange-correlation energy functional leads to the prediction of a quali-

tatively different type of behavior compared to LDA. GGA has a stronger formal foundation, because it accounts specifically for density gradients that are neglected in LDA, and does so in a way that satisfies several exact constraints on the form of the exchange-correlation energy functional. Put into practice, GGA seems to give a general improvement in comparison to experimental data for alkali metals, [8] 3d and 4d transition metals, [9] lanthanides, [10] and ionic insulators. [11] For covalent semiconductors the reports are somewhat inconclusive, [12] but overall GGA seems to be roughly as good as LDA. Assessing the differences between GGA and LDA is delicate, requiring in principle a full potential method. Because the GGA potential requires a more demanding calculation than does LDA, there are not yet many tests for multicomponent inter-metallic compounds.

The compound in question here is the Heusler compound Mn_2VAl . This compound is somewhat peculiar regardless of its detailed electronic structure: whereas there are many Heusler compounds of the form X_2YZ where $\text{Y}=\text{Mn}$, this compound is the only one reported where the X site is occupied by Mn. In the Y site Mn has high spin (around $4 \mu_B$ in X_2MnZ compounds [13]), while in the X site in Mn_2VAl it has been found in LDA calculations that it has a low spin, in agreement with measurements.

Although V and Al atoms may substitute on each other’s sublattice, in the system $\text{Mn}_2\text{V}_{1+x}\text{Al}_{1-x}$ the lattice constant and xray intensities show a kink at $x=0$, clearly identifying the stoichiometric composition. [14] The structure remains the Heusler one from x between -0.3 and +0.2, with linearly varying saturation moment. At stoichiometry the saturation moment is reported to be $1.9 \mu_B$, close to the integral value characteristic of the spin moment of HM magnets, [1,15] and the Curie temperature is $T_C = 760 \text{ K}$. The Curie constant obtained from high temperature susceptibility (above T_C) is consistent with the saturation moment. Nakamichi and Stager [16] inferred from NMR spin echo data that Mn and

V have moments near 1.2 and $-0.7 \mu_B$ respectively, making the net value ($2 \times 1.2 - 0.7$) roughly consistent with the reported saturation magnetization. Itoh *et al.* [17] obtained from neutron diffraction 1.5 ± 0.3 and $-0.9 \mu_B$ for Fe and V respectively.

Another reason for interest in this compound is the recent excitement caused by the related isostructural compound Fe_2VAl . From heat capacity, resistivity, and photoemission data this compound appears to be ‘chubby fermion’ metal, while LDA (and GGA) calculations [18–20] indicate that it has a semimetallic band structure with a very small number of carriers. One likely scenario is that its effective mass is enhanced by dynamic electron-hole correlations. [20]

In this paper we provide the results of accurate GGA calculations for Mn_2VAl . LDA calculations were presented earlier by Ishida, Asano, and Ishida [21], who obtained a near-HM situation that is reproduced by our LDA calculations. The important feature is that GGA predicts a HM FM (actually, ferrimagnetic, due to the moment of V that opposes the Mn moments). Recently there is increasing evidence that very large magnetoresistance and half-metallicity are closely related, for example in the ‘colossal magnetoresistance’ manganites [2] and in the double perovskite compound $\text{Sr}_2\text{MoRuO}_6$. [4] Due to this apparent close connection between HM behavior and large magnetoresistance, our predictions suggest that the magnetoresistance of Mn_2VAl should be measured. In Sec. II we describe the structure and outline our method of calculation. The results and comparison with Fe_2VAl are given in Sec. III. The conclusions are summarized in Sec. IV.

II. HEUSLER STRUCTURE, AND METHOD OF CALCULATION

Although the Heusler structural class includes an alloy system where the atoms on the Y and Z sites often intermix, indications are that at stoichiometry this compound corresponds to an ideal Heusler (L_{21}) structure compound. This structure type, pictured in Fig. 1, is based on an underlying bcc arrangement of atomic sites with lattice constant $a/2$, with V at $(0,0,0)$, Al at $(\frac{1}{2}, \frac{1}{2}, \frac{1}{2})a$, and Mn atoms at $(\frac{1}{4}, \frac{1}{4}, \frac{1}{4})a$ and $(\frac{3}{4}, \frac{3}{4}, \frac{3}{4})a$, where $a=5.875 \text{ \AA}$ is the lattice constant of the resulting fcc compound.

This structure is also that of Fe_2VAl and of Fe_3Al , the latter of which has two inequivalent Fe sites (X and Y sites). There is no report that Mn_3Al forms in this structure.

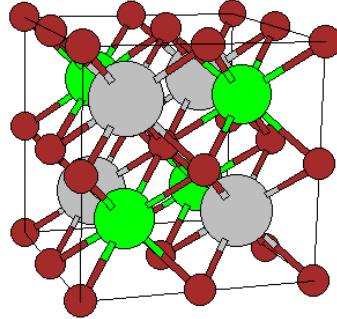


FIG. 1. The crystal structure of the Heusler compound Mn_2VAl . The small spheres denote the Mn sites, the medium and large spheres are the V and Al sites. The volume shown includes four primitive cells.

We have applied the linearized augmented plane wave method [22] that utilizes a fully general shape of density and potential. The WIEN97 code [23] has been used in the calculations. The lattice constant of 5.875 \AA was used. LAPW sphere radii (R) of 2.00 a.u. were chosen with cutoffs of RK_{max} up to 8.7 , providing well converged basis sets with more than 500 functions per primitive cell. Self-consistency was carried out on k -points meshes of around 200 points in the irreducible Brillouin zone ($12 \times 12 \times 12$ and $20 \times 20 \times 20$ meshes). The GGA exchange-correlation functional of Perdew *et al.* [7] was used in the present work.

III. DISCUSSION OF RESULTS

A. Ferrimagnetic Mn_2VAl

The majority and minority (which we will refer to as up and down) band structure resulting from GGA are shown in Fig. 2. These band structures are similar to what is obtained using LDA (see Ishida *et al.* [21]) except for the important difference that the gap in the majority bands at the Fermi level E_F is increased by 40% (from 0.25 eV to 0.35 eV). The position of E_F is essentially pinned by the minority band filling, and there is not any comparable band shifts in the minority bands within a few tenths of eV of E_F . The result of GGA, arising from the increase in the gap and the associated band rearrangements, is to empty the valence holes in the majority bands. The net (spin) magnetic moment is exactly $2 \mu_B$ per unit cell. The magnetic alignment is ferrimagnetic, with roughly a moment of $1.5 \mu_B$ on each Mn and $-0.9 \mu_B$ on V (see below for more discussion).

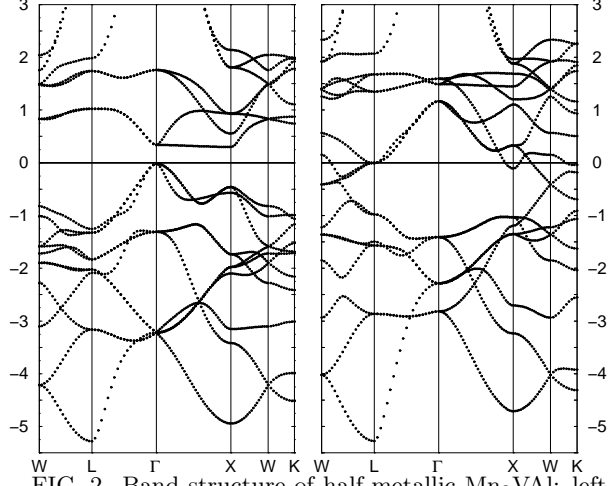


FIG. 2. Band structure of half-metallic Mn_2VAl : left panel, majority; right panel, minority. Note the extreme dissimilarity of the two sets of bands between -1 eV and 2 eV. One band, which is largely Al, lying below these bands in the -9 eV to -6 eV range, is not shown.

A very noticeable occurrence is just how different the majority and minority bands, shown in Fig. 2, are within 1 eV of E_F . In the majority bands the direct bandgap of 0.36 eV occurs at Γ ; in the minority bands the nearest bands to E_F are 1 eV away at Γ , both higher and lower. This difference, which is a drastic departure from simple Stoner exchange splitting, is related to ferrimagnetism, for which the exchange potentials are of opposite signs on the Mn and V atoms.

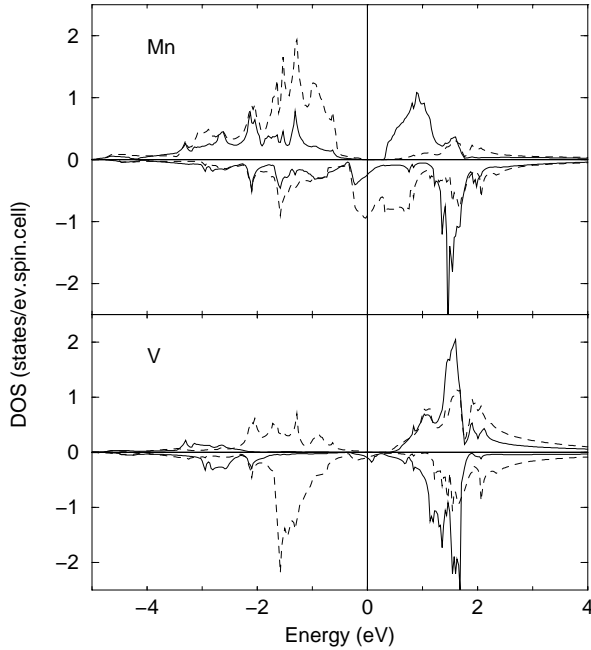


FIG. 3. Atom and symmetry projected density of states of Mn_2VAl , with majority plotted upward and minority plotted downward. e_g and t_{2g} symmetries are solid and dashed lines, respectively.

The atom and symmetry projected densities of states (PDOS) shown in Fig. 3 clarify the characters of the bands. The spin up bands below the gap are $\approx 80\%$ Mn, including all of the majority Mn t_{2g} states. Hence the Mn moment is strongly t_{2g} in character. Since for V only t_{2g} states are occupied in either spin channel, the V moment is also t_{2g} in character. The Al character is so small as to be difficult to see on the scale of Fig. 3, so it is not shown.

Above the gap lies most of the V spin up states, along with much of the Mn e_g states. In the spin down states below 0.5 eV, there are roughly equal amounts of V (t_{2g}) and Mn (mixed) states. Around E_F , however, the DOS is overwhelmingly Mn (strongly t_{2g}) in character. Hence the (100% polarized) charge carriers are associated almost entirely with Mn atoms.

The mechanism for antiparallel alignment of the V and Mn spins is not evident from our calculations. When parallel moments on V and Mn are used to begin the calculation, the V spin flips direction. This behavior suggests the FM alignment is substantially above the ferrimagnetic one in energy. Although it is tempting to speculate that the opening of the gap in the majority channel lowers the energy, which would provide a specific driving force toward half-metallicity, there is no particular evidence from our calculations to support such a scenario.

B. Fermi Surface

With the exception of positron annihilation studies of the half-Heusler compound NiMnSb , [24], Fermi surfaces of half metallic ferromagnets have not been directly measured, so we provide a brief description of the Fermi surface. The Fermi surface, which is of course solely for the minority bands, is rather interesting. It consists of small X-centered electron ellipsoids (nearly spherical) containing electrons, a large “jungle gym” type surface with arms along the cubic axes (Fig. 4), and a highly multiply-connected sheet that might be considered as centered at the L point of the Brillouin zone (Fig. 5). From Fig. 2, it can be seen that there is a near degeneracy of three bands (within 12 meV) that fall almost exactly at (actually straddle) the Fermi level.

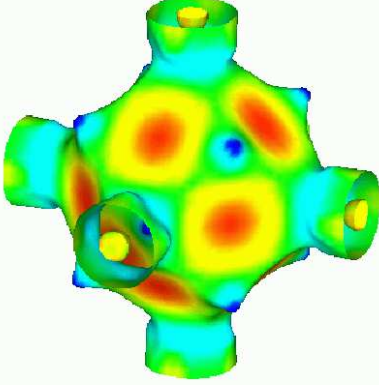


FIG. 4. Fermi surface of the lower band, which is of the general “jungle gym” type centered at Γ . There is also a tiny spheroid centered at the X points. The shading reflects the carrier velocity, which is smallest along the (111) directions and largest along the (110) direction.

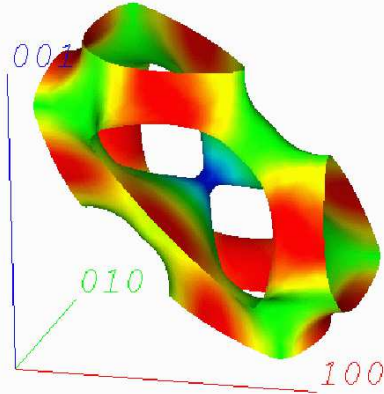


FIG. 5. Fermi surface of the higher band, with the cubic axes provided for orientation. This surface is multiply connected, with the L point (center of the hexagonal face) lying at the center of the portion that is shown (in one octant of the zone). The narrow neck at the L point is very sensitive to the Fermi level position.

This coincidence leads to identifiable structure in both Fermi surfaces. The jungle gym sheet has protrusions along the (111) direction very near the L point, while the surface in Fig. 5 has a narrow neck at the L point. The jungle gym also has flat regions perpendicular to the (110) directions that provide a nesting wavevector at $(0.85, 0.85, 0)\pi/a$ and symmetry related wavevectors. The surface in Fig. 5 has some flattish regions but no obvious strong nesting features.

C. Comparison with Fe_2VAL

Both from experiment and from the band structure, Fe_2VAL is vastly different from Mn_2VAL in spite

of its identical structure and closely related constituents. The total and projected DOS of Fe_2VAL is shown in Fig. 4 for comparison with Mn_2VAL . Fe_2VAL is a semimetal, practically a semiconductor, with a very deep and 1 eV wide pseudogap centered on the Fermi level. In fact, the majority bands of Mn_2VAL , which are isoelectronic with the majority bands of Fe_2VAL , have rather similar projected DOS, with the 1 eV pseudogap in Fe_2VAL becoming a 1.5 eV pseudogap with a true gap in the center for Mn_2VAL . The pseudogap in Fe_2VAL no doubt plays an important role in stabilizing the non-magnetic state in that compound.

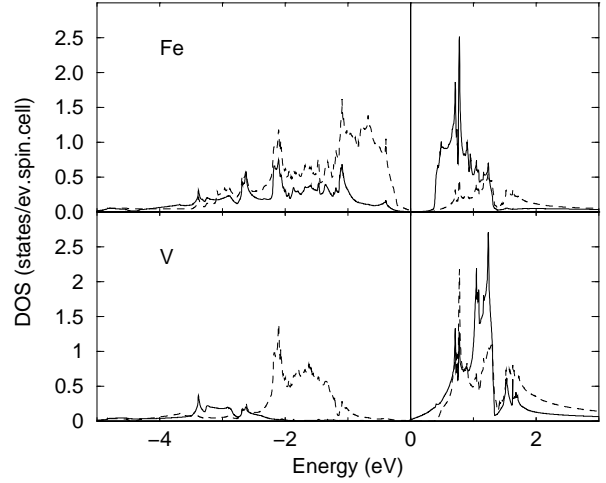


FIG. 6. Atom and symmetry projected density of states of Fe_2VAL from Ref. 15, plotted as in Fig. 3 except that this compound is non-magnetic. Comparison with Fig. 3 shows that the majority states of Mn_2VAL are comparable to Fe_2VAL , while the minority states of Fe/Mn differ strongly.

In the minority channel the electronic structures of the two compounds are quite distinct. Where in Fe_2VAL there is a pseudogap, in Mn_2VAL the X site (Mn) t_{2g} DOS is displaced to higher energies, and forms a partially occupied band with width ≈ 1.5 eV. This same Mn t_{2g} character in the majority shifts downward (from the exchange splitting) and is the cause of opening the majority spin band gap that leads to HM magnetism.

In Fe_2VAL the conduction band states just above E_F are purely V e_g in character. In Mn_2VAL the DOS within nearly 0.5 eV of the Fermi level, both above and below, are dominated by Mn t_{2g} character. The main onset of V e_g character has been pushed nearly 1 eV upward by the exchange splitting and the resulting changes in bonding.

IV. SUMMARY

We have shown that the GGA exchange-correlation functional leads to an increase of 40% (0.1 eV) in the bandgap in the majority bands leading to a HM band structure for Mn_2VAl , whereas LDA predicted band overlap in the majority channel. Since there is no reason to expect the structure in the high symmetry Heusler lattice to distort (and no distortion has been observed), and we have used the most advanced exchange-correlation functional known at present, this result represents a robust prediction of modern electronic structure theory. Since colossal magnetoresistance has been associated with the HM state in the ferromagnetic manganites and also apparently in the double perovskite $\text{Sr}_2\text{FeMoO}_6$, this compound gives another clear example to explore the relation between half-metallicity and large magnetoresistance.

V. ACKNOWLEDGMENTS

We acknowledge useful communication with E. Kurmaev. This work was supported by National Science Foundation Grant DMR-9802076. Figures 4 and 5 were produced by the AVS graphics package.

-
- [1] R. A. deGroot *et al.*, Phys. Rev. Lett. **50**, 2024 (1983); V. Yu. Irkhin and M. I. Katsnel'son, Usp. Fiz. Nauk **164**, 705 (1994) [Sov. Phys. Usp. **37**, 659 (1994)].
 - [2] J.-H. Park *et al.*, Nature **392**, 794 (1998).
 - [3] W. E. Pickett and D. J. Singh, Phys. Rev. B **53**, 1146 (1996).
 - [4] K.-I. Kobayashi, T. Kimura, H. Sawada, K. Terakura, and Y. Tokura, Nature **395**, 677 (1998).
 - [5] W. E. Pickett, Phys. Rev. B **57**, 10613 (1998)
 - [6] A structural distortion in the antiferromagnetic Heusler compound Fe_2VSi was reported by K. Endo, H. Matsuda, K. Ooiwa and K. Itoh, J. Phys. Soc. Japan **64**, 2329 (1995).
 - [7] J. P. Perdew *et al.*, Phys. Rev. B **46**, 6671 (1992); J. P. Perdew, K. Burke, and M. Ernzerhof, Phys. Rev. Lett. **77**, 3865 (1996).
 - [8] J. E. Jaffe, L. Zijing, and A. C. Hess, Phys. Rev. B **57**, 11834 (1998).
 - [9] K. Kokko and M. P. Das, J. Phys.: Cond. Matter **10**, 1285 (1998); R. Zeller, M. Asato, T. Hoshino, J. Zabloudil, P. Weinberger and P. H. Dederichs, Phil. Mag. B **78**, 417 (1998)..
 - [10] A. Delin, L. Fast, O. Eriksson and B. Johansson, J. Alloys and Compounds **275-277**, 472 (1998).
 - [11] J. K. Dewhurst, J. E. Lowther, and L. T. Madzwar, Phys. Rev. B **55**, 11003 (1997).
 - [12] C. Filippi, D. J. Singh, and C. J. Umrigar, Phys. Rev. B **50**, 14947 (1994); C. Stampfl and C. G. Van de Walle, Phys. Rev. B **59**, 5521 (1999); I.-H. Lee and R. M. Martin, Phys. Rev. B **56**, 7197 (1997); A. Dal Corso, A. Pasquarello, A. Baldereschi, and R. Car, Phys. Rev. B **53**, 1180 (1996).
 - [13] J. Kübler, A. R. Williams, and C. B. Sommers, Phys. Rev. B **28**, 1745 (1983).
 - [14] Y. Yoshida, M. Kawakami, and T. Nakamichi, J. Phys. Soc. Japan **50**, 2203 (1981).
 - [15] R. E. Rudd and W. E. Pickett, Phys. Rev. B **57**, 557 (1998).
 - [16] T. Nakamichi and C. V. Stager, J. Magn. Magn. Mater. **31-34**, 85 (1983).
 - [17] H. Itoh, T. Nakamichi, Y. Yamaguchi, and N. Kazama, Trans. Japan Inst. Metals **24**, 265 (1983).
 - [18] G. Y. Guo, G. A. Botton, and Y. Nishino, J. Phys.: Condens. Matter **10**, L119 (1998).
 - [19] D. J. Singh and I. I. Mazin, Phys. Rev. B **57**, 14352 (1998).
 - [20] R. Weht and W. E. Pickett, Phys. Rev. B **58**, 6855 (1998).
 - [21] S. Ishida, S. Asano, and J. Ishida, J. Phys. Soc. Japan **53**, 2718 (1984).
 - [22] D. J. Singh, *Planewaves, Pseudopotentials, and the LAPW Method* (Kluwer Academic, Boston, 1994).
 - [23] P. Blaha, K. Schwarz, and J. Luitz, WIEN97, Vienna University of Technology, 1997. Improved and updated version of the original copyrighted WIEN code, which was published by P. Blaha, K. Schwarz, P. Sorantin, and S. B. Trickey, Comput. Phys. Commun. **59**, 399 (1990).
 - [24] K. E. H. M. Hanssen and P. E. Mijnarends, Phys. Rev. B **34**, 5009 (1986); K. E. H. M. Hanssen, P. E. Mijnarends, L. P. L. M. Rabou, and K. H. J. Buschow, Phys. Rev. B **42**, 1533 (1990).